Density field in extended Lagrangian perturbation theory

Density field in extended Lagrangian perturbation theory

Takayuki Tatekawa*
Department of Physics, Waseda University, 3-4-1 Okubo, Shinjuku-ku, Tokyo 169-8555, Japan
(Received 13 September 2003; revised manuscript received 1 January 2004; published 20 April 2004)

We analyze the performance of a perturbation theory for nonlinear cosmological dynamics, based on the Lagrangian description of hydrodynamics. In our previous paper, we solved the hydrodynamic equations for a self-gravitating fluid with pressure, given by a polytropic equation of state, using a perturbation method. Then we obtained the first-order solutions in generic background universes and the second-order solutions for a wider range of polytrope exponents. Using these results, we describe density fields with a scale-free spectrum, SCDM, and LCDM models. Then we analyze the cross-correlation coefficient of the density field between *N*-body simulation and Lagrangian linear perturbation theory, and the probability distribution of the density fluctuations. From our analyses, for scale-free spectrum models, the case of the polytrope exponent 5/3 shows better performance than the Zel'dovich approximation and the truncated Zel'dovich approximation in the quasinonlinear regime. On the other hand, for SCDM and LCDM models, the improvement by including the effect of the velocity dispersion was small.

DOI: 10.1103/PhysRevD.69.084020 PACS number(s): 04.25.Nx, 95.30.Lz, 98.65.Dx

I. INTRODUCTION

The Lagrangian approximation for structure formation in cosmological fluids provides a relatively accurate model even in the quasilinear regime, where the density fluctuation becomes unity. The Zel'dovich approximation (ZA) [1–4], a linear Lagrangian approximation for a dust fluid, describes the evolution of density fluctuation better than the Eulerian approximation [5,6]. Although the ZA gives an accurate description until a quasilinear regime develops, it cannot describe the model after the formation of caustics. In the ZA, even after the formation of caustics, the fluid elements keep moving in the direction set up by the initial condition. The ZA cannot describe compact and high density structures such as pancakes, skeletons, or clumps, while *N*-body simulation shows the presence of clumps with a very wide range in mass at any given time [7]. In general, after the formation of caustics, the hydrodynamical description becomes invalid.

In order to proceed with a hydrodynamical description without the formation of caustics, the qualitative pressure gradient [8] and thermal velocity scatter [9,10] in a collisionless medium have been discussed. After that, the ''adhesion approximation'' [11] was proposed from the consideration of nonlinear wave equations like Burgers' equation. In the adhesion approximation, an artificial viscosity term is added to the ZA. As another modification, a Gaussian cutoff is applied to the initial power spectrum of the density fluctuation and then evolves with the ZA. This modified approximation is called the ''truncated Zel'dovich approximation'' (TZA) [12,13]. These modified approximations successfully avoid the formation of caustics and describe the evolution for long times. However, the physical origin of the modification has not been clarified.

We reconsider the basic, fundamental equation for the motion of matter. The collisionless Boltzmann equation [14] describes the motion of matter in phase space. The basic equations of hydrodynamics are obtained by integrating the collisionless Boltzmann equation over velocity space. In past approximations, such as the ZA and its modified version, velocity dispersion was ignored. Buchert and Domínguez [15] argued that the effect of velocity dispersion become important beyond the caustics. They also argued that models for large-scale structure should rather be constructed for a flow which describes the average motion of a multistream system. Then they showed that, when the velocity dispersion is still small and can be considered isotropic, that gives effective ''pressure'' or viscosity terms. Furthermore, they argued the relation between mass density ρ and pressure P, i.e., an ''equation of state.'' If the relation between the density of matter and pressure seems barotropic, the equation of state should take the form $P \propto \rho^{5/3}$. Buchert *et al.* [16] showed how the viscosity term is generated by the effective pressure of a fluid under the assumption that the peculiar acceleration is parallel to the peculiar velocity; Domínguez [17,18] clarified that a hydrodynamic formulation is obtained via a spatial coarse graining in a many-body gravitating system, and the viscosity term in the adhesion approximation can be derived by the expansion of coarse-grained equations.

Domínguez [19] also reported on a study of the spatially coarse-grained velocity dispersion in cosmological *N*-body simulations. The analysis showed that the polytrope exponent becomes $\gamma \simeq 5/3$ in a quasinonlinear regime, and $\gamma \simeq 2$ in a strongly nonlinear regime. Domínguez and Melott [20] discussed the polytrope exponents of velocity dispersion in *N*-body simulations. According to their results, the exponents depend on the model of the initial density fluctuation.

From these points, the extension of Lagrangian perturbation theory to cosmological fluids with pressure has been considered. Adler and Buchert [21] actually formulated the Lagrangian perturbation theory for a barotropic fluid. Morita and Tatekawa [22] and Tatekawa *et al.* [23] solved the Lagrangian perturbation equations for a polytropic fluid up to second order for cases where the equations are solved easily. Hereafter, we call this model the ''pressure model.''

*Electronic address: tatekawa@gravity.phys.waseda.ac.jp

In this paper, we analyze the density field which is described by the Lagrangian approximations; the ZA, TZA, and first-order pressure model solutions. We calculate the cross-correlation function of the density field between the Lagrangian approximation and *N*-body simulation. Furthermore, we analyze the probability distribution function of the density fluctuations for confirmation. From these results, we determine the polytrope exponent in the equation of state. From our analyses of the cross-correlation coefficient and probability distribution function of the density fluctuations, we find that the value of the polytrope exponent seems to be 5/3 for quasinonlinear evolution, as Buchert and Domínguez argued [15]. However, for the determination of the proportional constant in the equation of state, we must consider further physical processes or carry out a high-resolution *N*-body simulation.

This paper is organized as follows. In Sec. II, we present Lagrangian perturbative solutions. In Sec. II A, we show the first-order solution of the pressure model in the Einstein–de Sitter background. For comparison, in Secs. II B and II C, we show the solution of the ZA and the procedure of the TZA.

In Sec. III, we compare the density field between the Lagrangian approximations and *N*-body simulation. In Sec. III A, we calculate the cross-correlation coefficient of the density field. Although it seems that we can reach a conclusion in this analysis, it is insufficient. Therefore in Sec. III B, we analyze the probability distribution function of the density fluctuations. In Sec. IV, we discuss our results and state conclusions.

II. LAGRANGIAN APPROXIMATIONS IN GRAVITATIONAL INSTABILITY THEORY

A. First-order solutions of the pressure model

In this section, we present perturbative solutions in the Lagrangian description. The matter model we consider is a self-gravitating fluid with mass density ρ and ''pressure'' P, which is given by the presence of velocity dispersion. The ''pressure'' we adopt here is the same as was introduced by Buchert and Domínguez [15], i.e., the diagonal component of the velocity dispersion tensor when the velocity dispersion is assumed to be isotropic in the Jeans equation [14]. In Lagrangian hydrodynamics, the comoving coordinates $\boldsymbol{x}$ of the fluid elements are represented in terms of Lagrangian coordinates $\boldsymbol{q}$ as

$$\boldsymbol{x}=\boldsymbol{q}+\boldsymbol{s}(\boldsymbol{q},t), \tag{1}$$

where $\boldsymbol{q}$ are defined as initial values of $\boldsymbol{x}$, and $\boldsymbol{s}$ denotes the Lagrangian displacement vector due to the presence of inhomogeneities. From the Jacobian of the coordinate transformation from $\boldsymbol{x}$ to $\boldsymbol{q}$, $J\equiv\det(\partial x_i/\partial q_j)=\det(\delta_{ij}+\partial s_i/\partial q_j)$, the mass density is given exactly as

$$\rho=\rho_{\mathrm{b}}J^{-1}. \tag{2}$$

We decompose $\boldsymbol{s}$ into the longitudinal and the transverse modes as $\boldsymbol{s}=\nabla_{\boldsymbol{q}}S+\boldsymbol{S}^{\mathrm{T}}$ with $\nabla_{\boldsymbol{q}}\cdot\boldsymbol{S}^{\mathrm{T}}=0$. In this paper, we show the explicit form of the perturbative solutions only in the Einstein–de Sitter universe. For a generic background universe, we obtained the perturbation solutions in our previous paper [23].

The transverse modes can be solved easily. The first-order solutions become as follows:

$$\boldsymbol{S}^{\mathrm{T}}\propto a^0, a^{-1/2}. \tag{3}$$

Because the solutions do not depend on ''pressure,'' the solutions of this mode in the ZA become the same in form. The transverse modes do not have a growing solution in a first-order approximation.

For the longitudinal modes, we carry out a Fourier transformation with respect to the Lagrangian coordinates $\boldsymbol{q}$. If we assume a polytropic equation of state $P=\kappa\rho^{\gamma}$ with a constant κ and a polytrope exponent γ, we can write the explicit form of the first-order perturbative solutions. In the Einstein–de Sitter (EdS) background, the solutions are written in a relatively simple form. They are, for $\gamma\neq 4/3$,

$$\hat{S}(\boldsymbol{K},a)\propto a^{-1/4}\mathcal{J}_{\pm 5/(8-6\gamma)}\left(\sqrt{\frac{2C_2}{C_1}}\frac{|\boldsymbol{K}|}{|4-3\gamma|}a^{(4-3\gamma)/2}\right), \tag{4}$$

where $\mathcal{J}_{\nu}$ denotes the Bessel function of order ν, and for $\gamma=4/3$

$$\hat{S}(\boldsymbol{K},a)\propto a^{-1/4\pm\sqrt{25/16-C_2|\boldsymbol{K}|^2/2C_1}}, \tag{5}$$

where $C_1\equiv 4\pi G\rho_{\mathrm{b}}(a_{\mathrm{in}})a_{\mathrm{in}}^3/3$ and $C_2\equiv\kappa\gamma\rho_{\mathrm{b}}(a_{\mathrm{in}})^{\gamma-1}\times a_{\mathrm{in}}^{3(\gamma-1)}$. ρ_b and $\boldsymbol{K}$ are the background mass density and Lagrangian wave number, respectively. a_{in} is the scale factor when the initial condition was given.

Here we notice the relation between the behaviors of the above solutions and the Jeans wave number, which is defined as

$$K_{\mathrm{J}}\equiv\left(\frac{4\pi G\rho_{\mathrm{b}}a^2}{dP/d\rho(\rho_{\mathrm{b}})}\right)^{1/2}.$$

The Jeans wave number, which gives a criterion for whether a density perturbation with a wave number will grow or decay with oscillation, depends on time in general. If the polytropic equation of state $P=\kappa\rho^{\gamma}$ is assumed,

$$K_{\mathrm{J}}=\sqrt{\frac{3C_1}{C_2}}a^{(3\gamma-4)/2}. \tag{6}$$

Equation (6) implies that, if $\gamma<4/3$, K_{J} will be decreased and density perturbations with any scale will decay and disappear in evolution, and if $\gamma>4/3$, all density perturbations will grow to collapse. We rewrite the first-order solution Eq. (4) with the Jeans wave number:

$$\hat{S}(\boldsymbol{K},a)\propto a^{-1/4}\mathcal{J}_{\pm 5/(8-6\gamma)}\left(\frac{\sqrt{6}}{|4-3\gamma|}\frac{|\boldsymbol{K}|}{K_{\mathrm{J}}}\right). \tag{7}$$

B. Zel'dovich approximation

The ZA was obtained as the first-order solution with a dust fluid in the Lagrangian description [1]. The solutions are obtained from solutions of the pressure model at the limit of weak pressure. For example, in the EdS model, when we take the limit $\kappa \to 0$ in Eqs. (4) and (5), the solutions converge to those of the ZA:

$$\hat{S}(\boldsymbol{K},a) \propto a, a^{-3/2}. \tag{8}$$

The ZA is a perturbative solution that describes the structure well on a quasilinear scale. However, if caustics appear, the solutions no longer have physical meaning.

C. Truncated Zel'dovich approximation

During evolution, a small-scale structure contracts and forms caustics. Therefore if we introduce some cutoff in the small scale, we will be able to avoid the formation of caustics [12,13]. In the TZA, to avoid caustics, we introduce a Gaussian cutoff to the initial density spectrum as follows:

$$\mathcal{P}(k,t_{\rm in}) \to \mathcal{P}(k,t_{\rm in}) \exp(-k^2/k_{NL}), \tag{9}$$

where k_{NL} is the ''nonlinear wave number,'' defined by

$$1 = a(t)^2 \int_{k_0}^{k_{NL}} \mathcal{P}(k,t_{\rm in}) dk. \tag{10}$$

The nonlinear wave number depends on the scale factor. The relation between the Jeans wave number K_J and the nonlinear wave number k_{NL} will be discussed in Sec. IV.

III. COMPARISON BETWEEN *N*-BODY SIMULATION AND LAGRANGIAN APPROXIMATIONS

In this section, we show a comparison between *N*-body simulation and Lagrangian approximations with two statistical quantities. In our previous paper [23], we showed that the effect of second-order perturbation was still small just before shell crossing. Therefore we consider only first-order perturbations.

We analyze the ZA [1], the TZA [12,13], and the pressure model [21–23]. We establish the value of the scale factor at $z=0$ with $a=1$. For the initial condition, we set the Gaussian density field with the scale-free spectrum:

$$\mathcal{P}(k) \propto k^n (n=-1,0,1) \tag{11}$$

the standard cold dark matter (SCDM) and the low-density flat cold dark matter (LCDM) models). The initial condition was produced by COSMICS [24].

For *N*-body simulation, we execute the P^3M code. The parameters of the simulation were as follows: number of particles $N=64^3$, $N=128^3$ (Fig. 3 only); box size $L=64\ h^{-1}$ Mpc; softening length $\varepsilon=0.05\ h^{-1}$ Mpc; coarse-graining length $l=1,2,4\ h^{-1}$ Mpc; Hubble parameter $h=0.71$.

For CDM models, we choose the cosmological parameters as follows:

$$\text{SCDM:}\quad \Omega_m=1.0,\ \Omega_\Lambda=0.0,\ \sigma_8=0.84,$$

$$\text{LCDM:}\quad \Omega_m=0.27,\ \Omega_\Lambda=0.73,\ \sigma_8=0.84.$$

In the pressure model, we choose the polytrope exponent $\gamma=4/3,5/3$. In the case of $\gamma=4/3$, we obtain the simplest perturbative solution given by Eq. (5), which is described by a power law of the time variable. $\gamma=5/3$ is obtained from theoretical arguments by Buchert and Domínguez [15]. They argued kinematic considerations using the collisionless Boltzmann equation and derived $\gamma=5/3$. The exponent is equivalent to the adiabatic process of an ideal gas. Because we cannot decide on a proportionality constant κ in the equation of state from past discussion, we choose several values. In this paper, instead of κ, we write an initial ($a=10^{-3}$, i.e., $z=1000$) Jeans wave number, given by Eq. (6).

Here we show how we set up the initial condition in the pressure model. We adjust the initial condition in the pressure model to be the same as that in the ZA: the initial peculiar velocity in the pressure model is the same as that in the ZA. The procedure for setting up the initial condition was shown in our previous papers [22,23].

A. Cross-correlation coefficient

First we calculate the cross-correlation coefficient of the density fields. The cross-correlation coefficient was used for the comparison of the resulting density fields [12,13,25–28]. The cross-correlation coefficient is defined by

$$S \equiv \left\langle \frac{\delta_1 \delta_2}{\sigma_1 \sigma_2} \right\rangle, \tag{12}$$

where σ_i means the density dispersion of model i,

$$\sigma_i \equiv \sqrt{\langle \delta_i^2 \rangle}. \tag{13}$$

$S=1$ means that the patterns of the density fields of the two models coincide with each other. In the linear regime, the density dispersion remains $\sigma \ll 1$. Although we develop the structure until it becomes strongly nonlinear ($\sigma_{N\ \rm body} > 1$), we analyze it particularly in the quasinonlinear regime ($\sigma_{N\ \rm body} \simeq 1$).

Figures 1–6 show a comparison of *N*-body density fields with those predicted by various Lagrangian approximations. First, we notice the cases with a scale-free spectrum (Figs. 1–3). As in the past analyses, the TZA shows better performance than the ZA. Our analyses also show a similar tendency, i.e., our analyses do not contradict past analyses.

In the pressure model, the performance strongly depends on the polytrope exponent γ and the Jeans wave number. In the case of $\gamma=4/3$, when we set the initial Jeans wave number to be small, even if in the linear regime, the approximation deviates from an *N*-body simulation. Only for the case of $K_J=64$ does the approximation show better performance than the ZA in the quasinonlinear regime. We notice that the result strongly depends on the Jeans wave number in the case of $\gamma=4/3$: When we slightly change the value of the Jeans wave number, the cross-correlation coefficient changes dramatically. In the case of $\gamma=5/3$, although the result depends slightly on the initial Jeans wave number, the pressure model shows a better performance than the ZA in the quasinonlin-

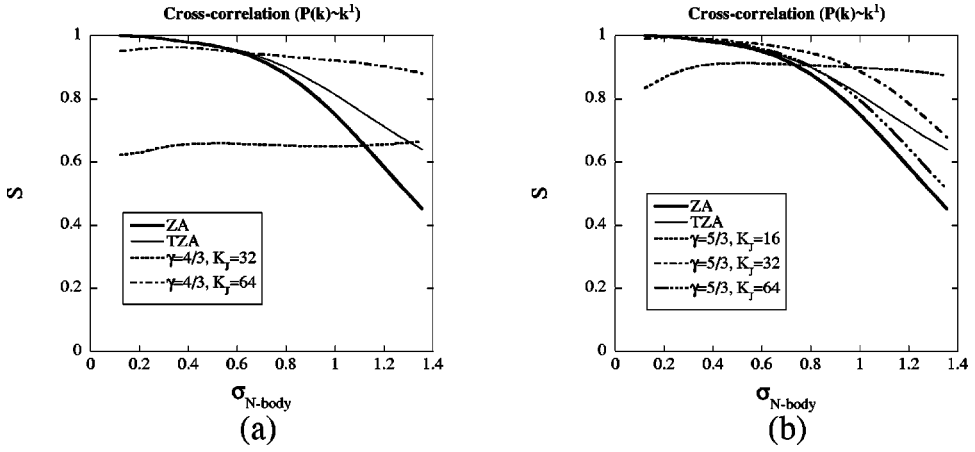

FIG. 1. The cross-correlation coefficient of density fields between the *N*-body simulation and Lagrangian approximations. The primordial density fluctuation is given by the scale-free spectrum $P(k)\propto k^1$ ($N=64^3, l=1\ h^{-1}$ Mpc). (a) When we choose $\gamma=4/3$, the function deviates from that of the ZA in the linear regime. (b) In the case of $\gamma=5/3$, we can obtain a better result than by using the TZA.

ear regime. Furthermore, the pressure model also shows a better performance than the TZA. However, when we consider scale-free spectrum models, the model does not have a typical physical scale: the model has only box size, grid size, and softening length. The trend of the result was unchanged when we changed the box size of the model and the softening parameter. When we changed the number of particles, the result changed. From a comparison of Figs. 1 and 3, we can see that the results depend on the ratio of grid size and initial Jeans wave number. In our calculation, we found that it was good to set up the value of κ so that the initial ($z=1000$) Jeans wave number K_J was $N^{1/3}/4\leqslant K_J\leqslant N^{1/3}$. For example, in the case of $N=64^3$, as we see in Figs. 1 and 2, it is good to choose the initial Jeans wave number $16\leqslant K_J\leqslant 64$.

Next we consider SCDM and LCDM models (Figs. 4–6). In these models, the difference between the ZA and TZA becomes very small. Because the initial density spectrum in the CDM models dumps power in the small scale, a cutoff in the spectrum weakly affects the formation of caustics, as we saw in the case of $P(k)\propto k^{-1}$. From Fig. 4, we can see that

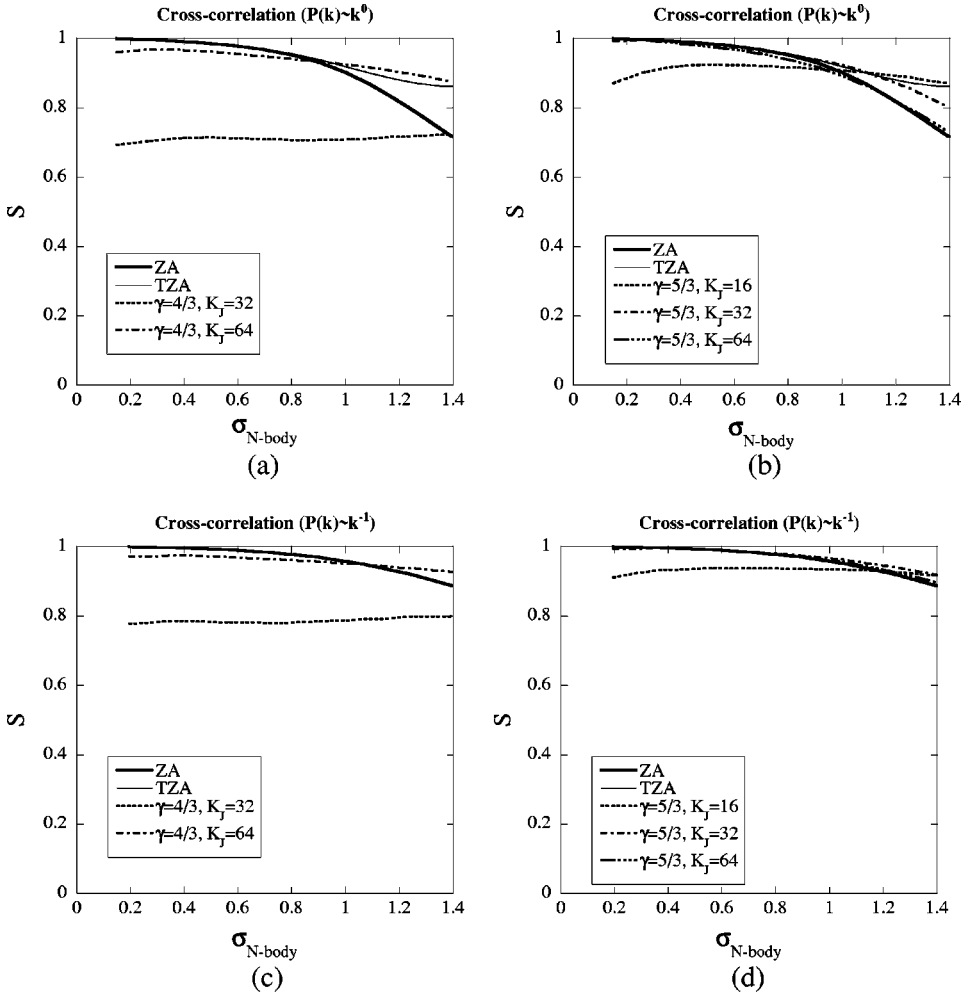

FIG. 2. The cross-correlation coefficient of density fields between the *N*-body simulation and Lagrangian approximations ($N=64^3, l=1\ h^{-1}$ Mpc, scale-free spectrum model). (a) $P(k)\propto k^0$, the case of $\gamma=4/3$. (b) $P(k)\propto k^0$, the case of $\gamma=5/3$. (c) $P(k)\propto k^{-1}$. In this model, the difference in the coefficient between the ZA and the TZA becomes small. The case of $\gamma=4/3$. (d) $P(k)\propto k^{-1}$, the case of $\gamma=5/3$.

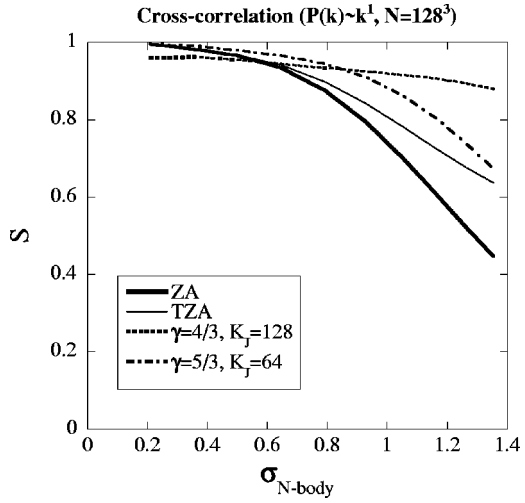

FIG. 3. The cross-correlation coefficient of density fields between *N*-body simulation and Lagrangian approximations. The primordial density fluctuation is given by the scale-free spectrum $P(k)\propto k^1$ ($N=128^3, l=1\ h^{-1}$ Mpc). From comparison between Fig. 1 and this graph, we can see that the results depend on the ratio of the grid size and initial Jeans wave number.

the effect of pressure improves the approximation in the quasinonlinear stage. Also, in both the SCDM and LCDM models, the case of $\gamma=4/3$ shows a deviation from the ZA in the linear regime. On the other hand, the case of $\gamma=5/3$ shows that the cross-correlation coefficient becomes almost the same in the linear regime. In the case of $\gamma=4/3$, when we choose a small initial Jeans wave number (for example, $K_J=16$), although we can improve the approximation much more in the quasinonlinear stage than at large Jeans wave number ($K_J=32,64$), the approximation changes slightly for the worse in the linear stage. On the other hand, when we choose $\gamma=5/3$, although the effect seems small, we can obtain an improved solution both in the linear and in the quasinonlinear stages.

When the model evolves to the strongly nonlinear regime, the trend of the solutions change. In the linear stage, the case of $\gamma=4/3$ shows deviation from the ZA. However, in the strongly nonlinear regime, although the Lagrangian approximation generally becomes worse, the case of $\gamma=4/3$ shows a rather good result [Figs. 4(a) and 4(c)]. This tendency was unchanged even when the coarse-graining length was changed (Figs. 5 and 6).

In both the SCDM and LCDM models, when we choose a small initial Jeans wave number K_J, although the approximation is improved after the quasinonlinear stage, the reasonable range of Jeans wave numbers seems wide. The strict limitation on the value of κ or the initial Jeans wave number will be given by other physical considerations or by a high-resolution *N*-body simulation.

From these results, we find that it is reasonable to choose the polytrope exponent $\gamma=5/3$ until the quasinonlinear re-

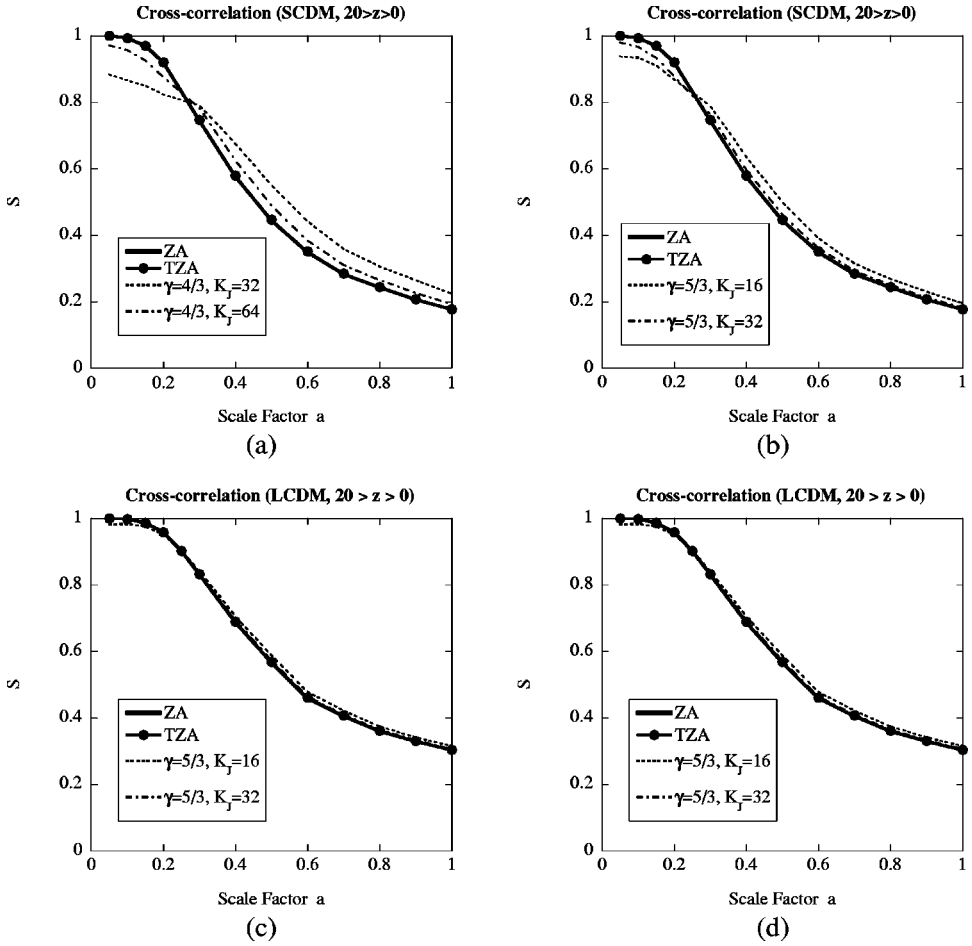

FIG. 4. The cross-correlation coefficient of density fields between an *N*-body simulation and Lagrangian approximations. The primordial density fluctuation is given by the CDM spectrum ($N=64^3, l=1\ h^{-1}$ Mpc). Models in which hardly any difference appears are excluded from the graph. (a) The SCDM model with $\gamma=4/3$. (b) The SCDM model with $\gamma=5/3$. (c) The LCDM model with $\gamma=4/3$. (d) The LCDM model with $\gamma=5/3$.

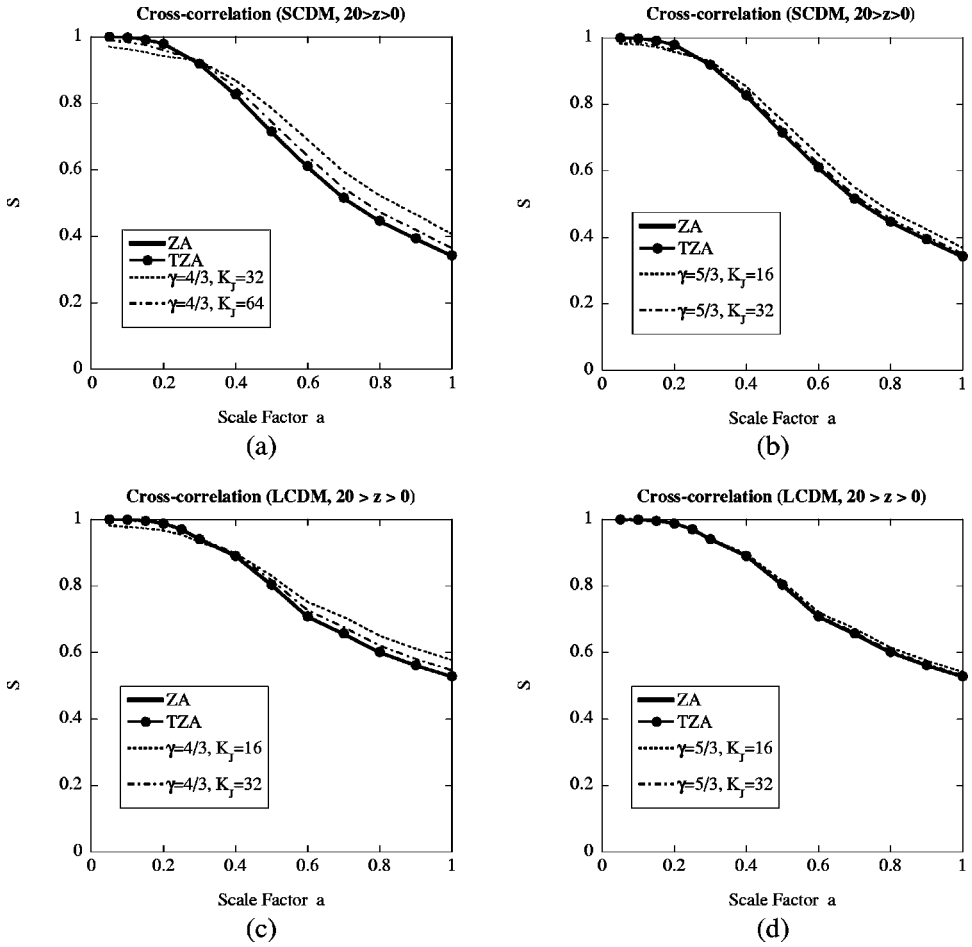

FIG. 5. The same as Fig. 4. In these figures, we changed the coarse-graining length to $l = 2\ h^{-1}$ Mpc. (a) The SCDM model with $\gamma = 4/3$. (b) The SCDM model with $\gamma = 5/3$. (c) The LCDM model with $\gamma = 4/3$. (d) The LCDM model with $\gamma = 5/3$.

gime is reached. These results support the suggestion by Buchert and Domínguez [15] and by Domínguez [19]. If we have interest in the strongly nonlinear regime, although the Lagrangian approximation generally becomes worse, we had better analyze the case of $\gamma = 4/3$. In this regime, it is necessary to consider whether that approximation will still be valid. In any case, from the cross-correlation coefficient, we can put limitations on the polytrope exponent γ.

Unfortunately, in these results, we cannot give a strict limit to the proportionality coefficient κ of the equation of state. When we choose $\gamma = 4/3$, we show that the result strongly depends on κ, and we can see a strict limitation. However, when we choose $\gamma = 5/3$, we can hardly judge the best value for κ. In our calculation, we found that it was good to set up the initial ($a = 10^{-3}$, i.e., $z = 1000$) Jeans wave number K_J as $N^{1/3}/4 \leqslant K_J \leqslant N^{1/3}$. From the range of K_J, we can obtain a reasonable value for κ. If we choose a large value for κ, it becomes hard to form a nonlinear structure. On the other hand, if we choose a small value for κ, the structure becomes almost the same as the structure that was obtained by the ZA.

Although the cross-correlation coefficient is one thing which is good for checking the accuracy of the approximation, it is not enough. Now we consider two samples A and B. The density contrast of the samples is given by δ_A and δ_B, respectively. We assume that the following proportionality relation exists between δ_A and δ_B:

$$\delta_A \propto \delta_B . \tag{14}$$

Even if the density contrast is greatly different, as given by δ_A and δ_B, and one shows a highly nonlinear structure and the other remains in the linear regime, the cross-correlation coefficient between δ_A and δ_B becomes 1.

Therefore, we must check the accuracy of the approximation using another property. In the next subsection, we analyze the probability distribution function of the density fluctuations.

B. Probability distribution function of density fluctuation

Here, we compare the probability distribution function (PDF) of the density fluctuations. In the Eulerian linear approximation, if initial data are given by a random Gaussian distribution, the PDF of density fluctuations will retain its Gaussianity during evolution. On the other hand, in the Lagrangian approximation, a nonlinear effect appears. In fact, Kofman *et al.* [29] show that the PDF of the density fluctuations approaches a log-normal function rather than a Gaussian function in the cases of the Lagrangian approximation and N-body simulation. Padmanabhan and Subramanian [30] also discussed the PDF of density fluctuations with the ZA and found a non-Gaussian distribution.

How will the PDF of the density fluctuations change if we take the effect of the velocity dispersion into consideration?

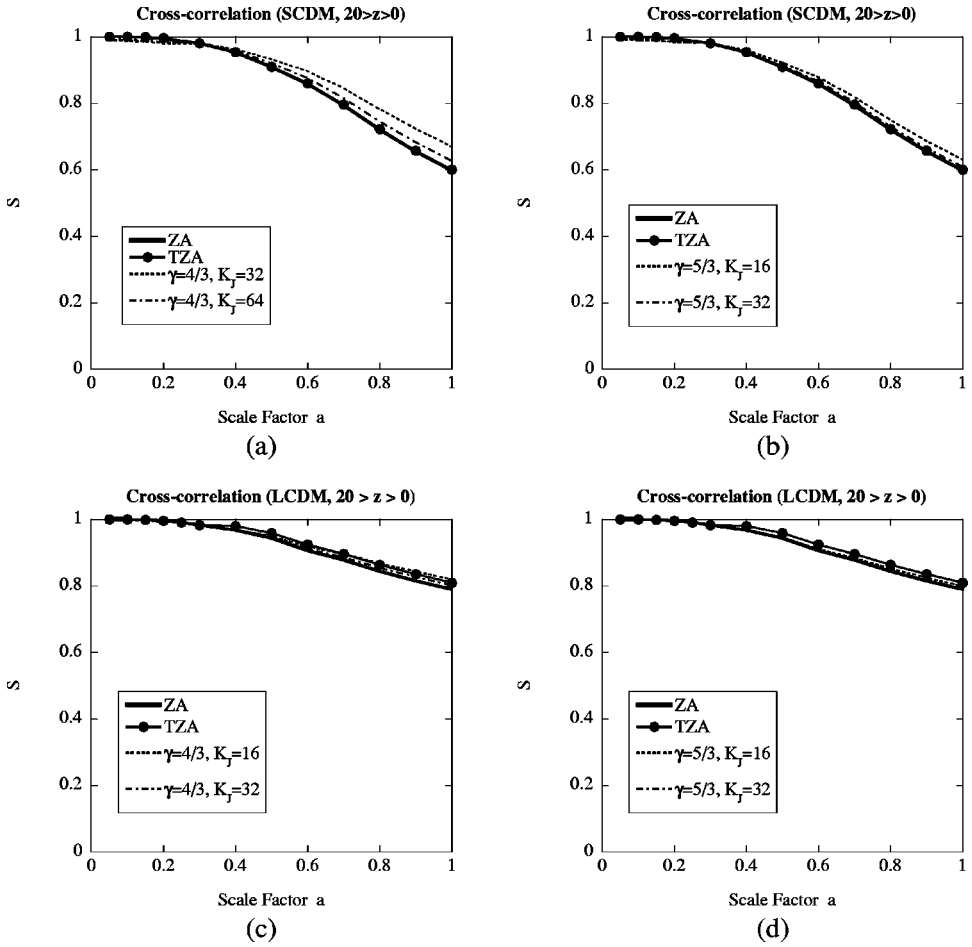

FIG. 6. The same as Fig. 4. In these figures, we changed the coarse-graining length to $l = 4\ h^{-1}$ Mpc. (a) The SCDM model with $\gamma = 4/3$. (b) The SCDM model with $\gamma = 5/3$. (c) The LCDM model with $\gamma = 4/3$. (d) The LCDM model with $\gamma = 5/3$.

Figures 7, 8, and 9 show the PDFs of the density fluctuations. As in past work, the PDF of the density fluctuations becomes log-normal in form in the *N*-body simulation. In Figs. 7, 8, and 9, the cases of $\gamma = 4/3$ obviously show a different tendency: in these cases, the effect of pressure suppresses the growth of positive fluctuations [Figs. 7(b), 8(c), 8(d), 9(c), and 9(d)]. When we also consider the PDF of density fluctuations, we can see that it is not so good to choose $\gamma = 4/3$ to examine the growth of structure, although the cross-correlation coefficients show the trend well. On the other hand, the case of $\gamma = 5/3$ well shows the trend in the PDF of the density fluctuations. Although the difference of distribution between the ZA and the pressure model is still small in the quasinonlinear regime, the effect of the pressure can promote the evolution of nonlinear structure. Therefore the probability of low- and high-density regions increases in the case of $\gamma = 5/3$. Furthermore, according to Fig. 8(c), the PDFs of density fluctuations in the cases of $\gamma = 5/3$ show that it is much better than the result in the TZA case. Of course when we reach a strongly nonlinear regime, it is necessary to

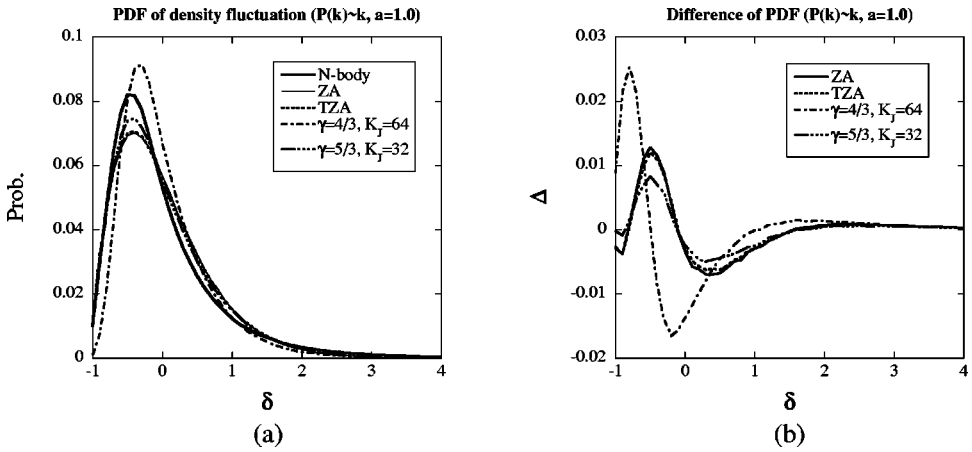

FIG. 7. The PDF of density fluctuation for a scale-free spectrum ($P(k) \propto k$, $l = 1\ h^{-1}$ Mpc: $\sigma_{N\ \mathrm{body}} \simeq 1$ at $a = 1.0$.). (a) The PDF of density fluctuation. In the case of $\gamma = 4/3$, the effect of pressure suppresses the growth of the fluctuation. (b) The difference in the PDF of density fluctuation. In this figure, the difference between the case of $\gamma = 4/3$ and other cases becomes clear. When we choose $K_J = 32$ for the case of $\gamma = 4/3$, more greater difference appears.

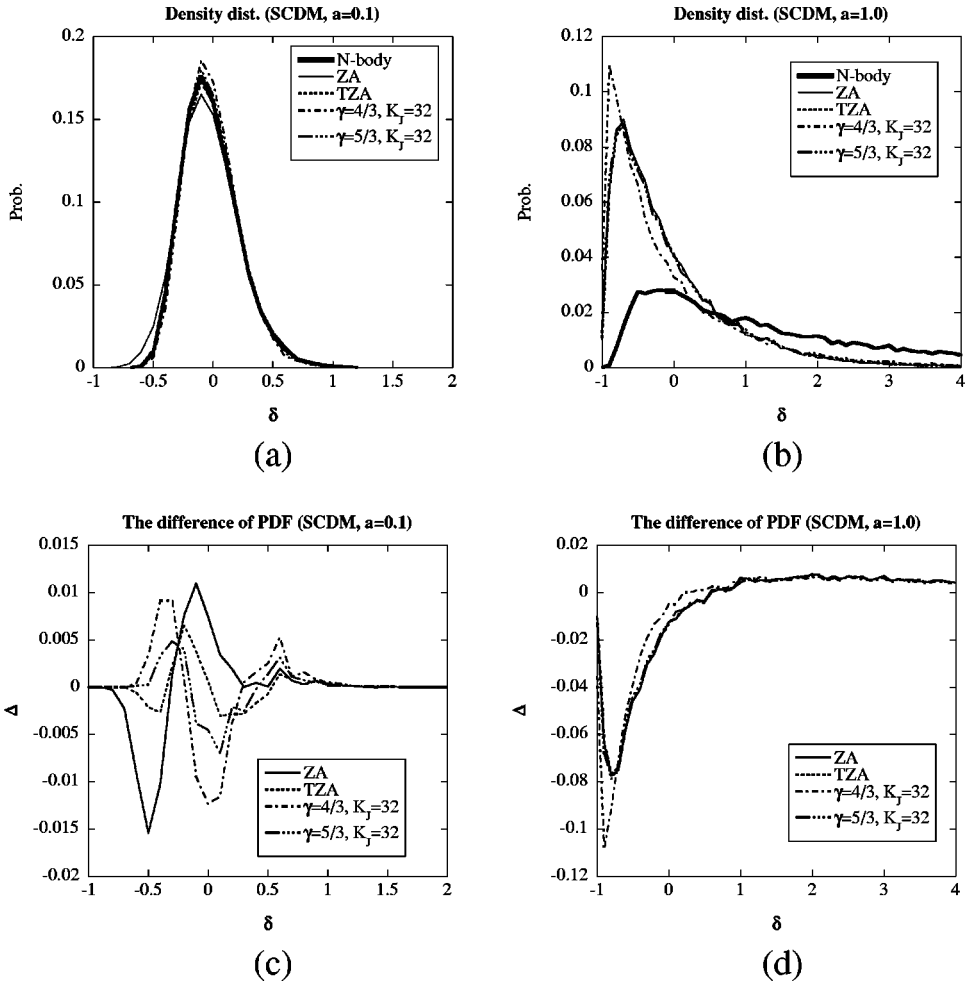

FIG. 8. The PDF of density fluctuations in the SCDM model ($l=4\ h^{-1}$ Mpc). In the case of $\gamma=4/3$, the pressure effect suppresses the growth of density fluctuations. Therefore the probability of a small fluctuation ($|\delta|<1$) increases. (a) The SCDM model at $a=0.1$ ($z=9$, $l=4\ h^{-1}$ Mpc, quasinonlinear regime). In the case of $\gamma=4/3$, the effect of pressure suppresses the growth of the fluctuation. (b) The SCDM model at $a=1.0$ ($z=0$, $l=4\ h^{-1}$ Mpc, strongly nonlinear regime). (c) The difference in the PDFs of density fluctuations between the *N*-body simulation and Lagrangian approximations at $a=0.1$. (d) Same as (c), but at $a=1.0$.

consider whether or not that approximation is still valid.

From both the cross-correlation coefficient and PDF of the density fluctuations, we can decide that it is reasonable to choose $\gamma=5/3$ as the polytrope exponent of the equation of state. However, it is hard to decide the proportionality parameter κ. From the results in this paper, we cannot give a tight limit to κ. To decide the value of κ, we will analyze a high-resolution *N*-body simulation or consider other physical processes. For example, we will consider the effect of the anisotropic velocity dispersion [32] or the higher-order velocity cumulant.

IV. DISCUSSION AND CONCLUDING REMARKS

We compared two statistical quantities between an *N*-body simulation and Lagrangian approximations. In our earlier work [22,23], we solved the first-order perturbation equations in a homogeneous and isotropic background and the second-order ones explicitly for the case $\gamma=4/3,5/3$ in an Einstein–de Sitter universe. We showed that the difference between the Lagrangian first-order and second-order approximations becomes small in the case of $\gamma\geqslant 4/3$. Therefore, in this paper we considered only the first-order perturbative solution for the case $\gamma=4/3,5/3$. Then we carried out a similar calculation with the ZA and TZA to examine their difference from the previous models.

First, we compared these models using the cross-correlation coefficient of the density field between the *N*-body simulation and Lagrangian approximations. In scale-free spectrum cases, as well as in the previous analyses, the TZA shows a better performance than the ZA. In the pressure model, the performance strongly depends on the polytrope exponent γ and the Jeans wave number. In the case of $\gamma=4/3$, when we set that initial Jeans wave number to be small, even in the linear regime the approximation deviates from the *N*-body simulation. In the case of $\gamma=5/3$, although the result slightly depends on the initial Jeans wave number, the pressure model shows a better performance than the ZA in the quasinonlinear regime. Furthermore, the pressure model also shows better performance than the TZA. In the SCDM and LCDM models, the case of $\gamma=4/3$ shows deviation from the ZA in the linear regime. On the other hand, the case of $\gamma=5/3$ shows that the cross-correlation coefficient becomes almost the same in the linear regime. When the model reaches a strongly nonlinear stage, although the Lagrangian approximation generally becomes worse, the case of $\gamma=4/3$ shows a rather good result. Of course, in this regime, it is necessary to consider whether that approximation is still valid.

Second, we analyzed the PDF of the density fluctuations. The case of $\gamma=4/3$ obviously shows a different tendency

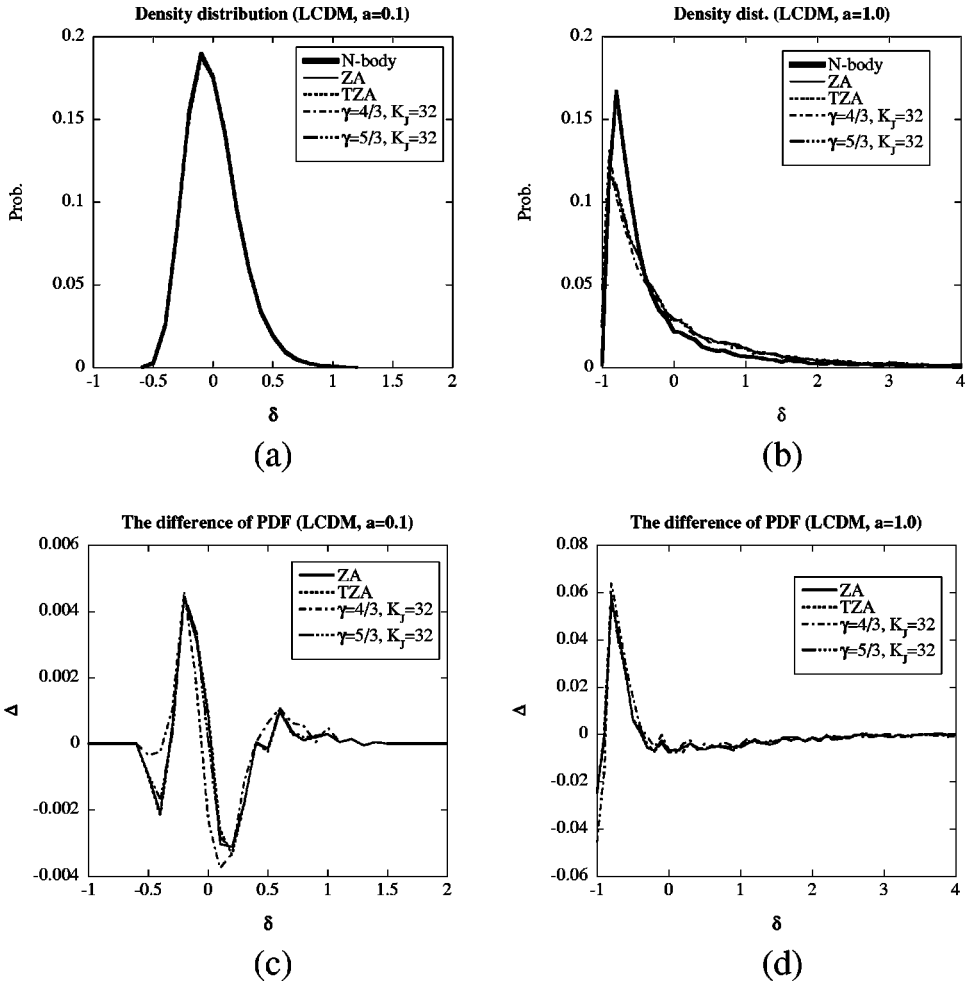

FIG. 9. The PDF of density fluctuations in the LCDM model ($l=4\ h^{-1}$ Mpc). In the case of $\gamma=4/3$, the pressure effect suppresses the growth of density fluctuations. Therefore the probability of a small fluctuation ($|\delta|<1$) increases. (a) At $a=0.1$ ($z=9$, $l=4\ h^{-1}$ Mpc, quasinonlinear regime). The PDFs of density fluctuations seem similar to each other. (b) At $a=1.0$ ($z=0$, $l=4\ h^{-1}$ Mpc, strongly nonlinear regime). (c) The difference in the PDFs of density fluctuations between the *N*-body simulation and Lagrangian approximations at $a=0.1$. (d) Same as (c), but at $a=1.0$.

until the quasinonlinear regime is reached: in this case, the effect of pressure suppresses the growth of structure. When we also consider the probability distribution of the density, we can see that it is not so good to choose $\gamma=4/3$ to examine the growth of structure, although the cross-correlation coefficients perform well. On the other hand, the case $\gamma=5/3$ shows good tendencies in the PDFs of the density fluctuations. Although the difference of the PDFs of the density fluctuations between the ZA and the pressure model is still small in the quasinonlinear regime, the effect of the pressure can promote the evolution of nonlinear structure. The difference between the models of Lagrangian approximation becomes small when we calculate the evolution until the strongly nonlinear regime is reached. From analyses of the cross-correlation coefficient of the density field and the PDF of the density fluctuations, we can decide that it is reasonable to choose $\gamma=5/3$ as the polytrope exponent of the equation of state.

In this paper, we changed some values of the Jeans wave number K_J and undertook the analysis. Are there any relations between the nonlinear wave number k_{NL} in the TZA and K_J? The correspondence is as follows. For simplification, we consider the correspondence in the case of a scale-free spectrum $P(k)\propto k^n$. According to the definition of the nonlinear wave number in the TZA, k_{NL} is given from Eq. (10). In the case of the scale-free spectrum $P(k)=Ak^n$, the definition becomes

$$\frac{1}{n+1}a(t)^2Ak_{NL}^{n+1}=1. \tag{15}$$

From this definition, k_{NL} is written as

$$k_{NL}\sim a^{-2/(1+n)}. \tag{16}$$

For example, when we choose $n=1$, k_{NL} becomes

$$k_{NL}\sim\frac{1}{a}. \tag{17}$$

On the other hand, the Jeans wave number K_J in the pressure model is given from Eq. (6). When we choose $\gamma=2$, K_J becomes

$$K_J\sim\frac{1}{a}. \tag{18}$$

There are some different points to consider when we think about the time evolution, although the relation seems to be as described above. First, in the TZA, k_{NL} affects only the initial spectrum. On the other hand, K_J affects the evolution of

fluctuations. Second, although k_{NL} obviously depends on the initial spectrum, we did not clarify the dependence on the initial condition of K_J. We think that a consideration of the physical process, which was not considered here, or the analysis of the *N*-body simulation, is necessary for a decision about K_J, i.e., κ. We will have to think about the correspondence between the adhesion approximation and the pressure model. Buchert *et al.* [16] showed how the viscosity term in the adhesion approximation is generated by a pressurelike force. Domínguez [17,18] discussed spatial coarse graining in a gravitating system and derived an evolution equation for the adhesion approximation. We showed that the density distribution of the pressure model was similar to that of the TZA in a previous paper [23]. The acute characteristic skeleton structure which appeared in the adhesion approximation could not be seen from the calculations in our previous paper. We will consider the relation between the viscosity term in the coarse-grained equations and the pressure term in our model. Then we will analyze the correspondence between the viscosity term in the adhesion approximation and the proportionality constant κ in the equation of state in the pressure model.

In this paper, we analyzed only the density distribution. How will the peculiar velocity distribution change with the effect of ''pressure''? In the ZA, the peculiar velocity is in proportion to the Lagrangian displacement. Then the growth rate of perturbations is independent of scale. Therefore, although the structure reaches the nonlinear regime, if the initial condition is given as Gaussian, the peculiar velocity distribution remains Gaussian all the time [29]. However, in the pressure model, the growth rate of the perturbation depends on the scale. Therefore the peculiar velocity distribution will deviate from Gaussian during the evolution. Of course, the peculiar velocity distribution in an *N*-body simulation becomes non-Gaussian [31]. Does the effect of the pressure cause the occurrence of the non-Gaussian distribution? We think that the time evolution of the peculiar velocity distribution is one of the more interesting problems.

In our model, we introduce the strong simplification that the velocity dispersion is approximately isotropic, i.e., the stress tensor is diagonal and has a pressurelike term [16]. However, in general, the velocity dispersion does not remain isotropic in the nonlinear regime. Until when is the assumption to ignore anisotropic velocity dispersion reasonable? Maartens *et al.* [32] discussed a relativistic kinetic theory generalization which also incorporates an anisotropic velocity dispersion. Then they added these effects to the linear development of density inhomogeneity and found exact solutions for their evolution. In a Newtonian description, although the equations are not generally closed, we will consider an anisotropic velocity dispersion and the higher-order velocity cumulant and estimate their effects on the evolution of density inhomogeneity.

ACKNOWLEDGMENTS

We would like to thank Thomas Buchert, Kei-ichi Maeda, Masaaki Morita, Momoko Suda, and Hideki Yahagi for useful discussions and comments on the work. For usage of COSMICS and P^3M codes, we would like to thank Edmund Bertschinger and Alexander Shirokov. This work was supported in part by a Waseda University Grant for Special Research Projects (Individual Research 2002A-868 and 2003A-089).

[1] Ya.B. Zel'dovich, Astron. Astrophys. **5**, 84 (1970).
[2] T. Buchert, Mon. Not. R. Astron. Soc. **254**, 729 (1992).
[3] P. Coles and F. Lucchin, *Cosmology: The Origin and Evolution of Cosmic Structure* (John Wiley & Sons, Chichester, England, 1995).
[4] V. Sahni and P. Coles, Phys. Rep. **262**, 1 (1995).
[5] D. Munshi, V. Sahni, and A.A. Starobinsky, Astrophys. J. **436**, 517 (1994).
[6] V. Sahni and S.F. Shandarin, Mon. Not. R. Astron. Soc. **282**, 641 (1996).
[7] M. Davis, G. Efstathiou, C.S. Frenk, and S.D.M. White, Astrophys. J. **292**, 371 (1985).
[8] Ya.B. Zel'dovich, Sov. Astron. **26**, 289 (1982).
[9] É.V. Kotok and S.F. Shandarin, Sov. Astron. **31**, 600 (1987).
[10] S.F. Shandarin and Ya.B. Zel'dovich, Rev. Mod. Phys. **61**, 185 (1989).
[11] S.N. Gurbatov, A.I. Saichev, and S.F. Shandarin, Mon. Not. R. Astron. Soc. **236**, 385 (1989).
[12] P. Coles, A.L. Melott, and S.F. Shandarin, Mon. Not. R. Astron. Soc. **260**, 765 (1993).
[13] A.L. Melott, T.F. Pellman, and S.F. Shandarin, Mon. Not. R. Astron. Soc. **269**, 626 (1994).
[14] J. Binney and S. Tremaine, *Galactic Dynamics* (Princeton University Press, Princeton, NJ, 1987).
[15] T. Buchert and A. Domínguez, Astron. Astrophys. **335**, 395 (1998).
[16] T. Buchert, A. Dom⁂uez, and J. Perez-Mercader, Astron. Astrophys. **349**, 343 (1999).
[17] A. Domínguez, Phys. Rev. D **62**, 103501 (2000).
[18] A. Domínguez, Mon. Not. R. Astron. Soc. **334**, 435 (2002).
[19] A. Domínguez, Astron. Nachr. **324**, 560 (2003).
[20] A. Domínguez and A.L. Melott, astro-ph/0310693.
[21] S. Adler and T. Buchert, Astron. Astrophys. **343**, 317 (1999).
[22] M. Morita and T. Tatekawa, Mon. Not. R. Astron. Soc. **328**, 815 (2001).
[23] T. Tatekawa, M. Suda, K. Maeda, M. Morita, and H. Anzai, Phys. Rev. D **66**, 064014 (2002).
[24] E. Bertschinger, Astrophys. J., Suppl. Ser. **137**, 1 (2001).
[25] A.L. Melott, S.F. Shandarin, and D.H. Weinberg, Astrophys. J. **428**, 28 (1994).
[26] T. Buchert, A.L. Melott, and A.G. Weiss, Astron. Astrophys. **288**, 349 (1994).
[27] A.L. Melott, T. Buchert, and A.G. Weiss, Astron. Astrophys. **294**, 345 (1995).
[28] G. Karakatsanis, T. Buchert, and A.L. Melott, Astron. Astrophys. **326**, 873 (1997).

[29] L. Kofman, E. Bertschinger, J.M. Gelb, A. Nusser, and A. Dekel, Astrophys. J. **420**, 44 (1994).
[30] T. Padmanabhan and K. Subramanian, Astrophys. J. **410**, 482 (1993).
[31] W.H. Zurek, P.J. Quinn, J.K. Salmon, and M.S. Warren, Astrophys. J. **431**, 559 (1994).
[32] R. Maartens, J. Triginer, and D.R. Matravers, Phys. Rev. D **60**, 103503 (1999).